Check for updates

How to cite: *Angew. Chem. Int. Ed.* **2022,** *61,* e202211496
International Edition: doi.org/10.1002/anie.202211496
German Edition: doi.org/10.1002/ange.202211496

Carbenes

N-Heterocyclic Carbene-Assisted Reversible Migratory Coupling of Aminoborane at Magnesium

Akachukwu D. Obi, Nathan C. Frey, Diane A. Dickie, Charles Edwin Webster, and Robert J. Gilliard Jr**

Abstract: A combined synthetic and theoretical investigation of N-heterocyclic carbene (NHC) adducts of magnesium amidoboranes is presented, which involves a rare example of reversible migratory insertion within a normal valent *s*-block element. The reaction of (NHC)Mg(N(SiMe$_3$)$_2$)$_2$ (**1**) and dimethylamine borane yields the tris(amide) adduct (NHC–BN)Mg(NMe$_2$BH$_3$)(N(SiMe$_3$)$_2$) (**2**; NHC–BN = NHC–BH$_2$NMe$_2$). In addition to Me$_2$N=BH$_2$ capture at the ^{NHC}C–Mg bond, mechanistic investigations suggest the likelihood of aminoborane migratory insertion from an RMg(NMe$_2$BH$_2$NMe$_2$BH$_3$) intermediate. To elucidate these processes, the carbene complexes (NHC)Mg(NMe$_2$BH$_3$)$_2$ (**8**) and (NHC)Mg(NMe$_2$BH$_2$NMe$_2$BH$_3$)$_2$ (**9**) were synthesized, and a dynamic migration of Me$_2$N=BH$_2$ between Mg–N and ^{NHC}C–Mg bonds was observed in **9**. This unusual reversible migratory insertion is presumably induced by dissimilar charge localization in the $^-${NMe$_2$BH$_2$NMe$_2$BH$_3$} anion, as well as the capacity of NHCs to reversibly capture Me$_2$N=BH$_2$ in the presence of Lewis acidic magnesium species.

Introduction

The promise of ammonia borane (NH_3BH_3) for hydrogen storage is punctuated by its slow dehydrogenation kinetics and formation of undesirable by-products such as borazine (a fuel-cell poison) and ceramic boron nitride.[1–9] As an alternative, saline *s*-block metal amidoboranes [M-(NH$_2$BH$_3$)$_x$; M = Li, Na, K, Mg, Ca, Sr; x = 1 or 2] are capable of thermal dehydrogenation under much milder conditions than NH_3BH_3, with little to no borazine release.[10–20] In addition, their molecular complexes are competent for catalytic amine borane dehydrogenation (Figure 1a),[21–26] even under ambient conditions.[23] The apparent catalytic activity trend for simple *s*-block M(N(SiMe$_3$)$_2$)$_x$ complexes is Mg > Li ≈ Na > K ≈ Ca,[24] but highly variable activity can be achieved by rational modification of their coordination environments.[21–23] Significantly, these molecular complexes are amenable to structural, electronic and mechanistic analyses,[5] which complement solid-state mass or volumetric analysis techniques[2,7] for a holistic understanding of amine borane dehydrogenation.

Divalent group 2 metals are privileged to support a well-defined Ae–NR$_2$BH$_3$ unit (Ae = alkaline earth metal) kinetically stabilized by a persistent, monoanionic ligand with significant steric demand (e.g., β-diketiminate).[25–28] Consequently, they provide a molecular platform for probing metal–hydride polarizations, secondary interactions, and intermediates of thermal or catalytic dehydrogenation reactions through ^{11}B NMR spectroscopy and X-ray crystallography.[25–31] Conversely, solution-state investiga-

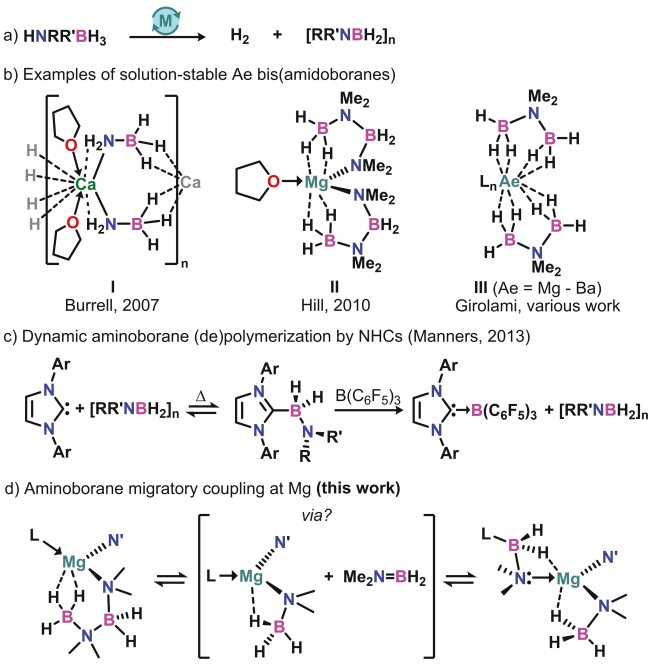

Figure 1. a) Simplified catalytic amine borane dehydrogenation by molecular species (R, R′ = H, alkyl, aryl). b) Select examples of solution-stable group 2 bis(amidoboranes). c) Dynamic depolymerization of aminoboranes by N-heterocyclic carbenes (NHCs). d) This work: NHC-assisted reversible migratory insertion of aminoborane at magnesium (L = NHC, N′ = silylamide or amidoborane).

[*] A. D. Obi, N. C. Frey, Dr. D. A. Dickie, Prof. Dr. R. J. Gilliard Jr
Department of Chemistry, University of Virginia
409 McCormick Road, PO Box 400319,
Charlottesville, VA 22904 (USA)
E-mail: rjg8s@virginia.edu
Prof. Dr. C. E. Webster
Department of Chemistry, Mississippi State University
PO Box 9573, Mississippi State, MS 39762 (USA)
E-mail: ewebster@chemistry.msstate.edu

© 2022 Wiley-VCH GmbH

tions of homoleptic $Ae(NR_2BH_3)_2$ complexes are sparse. With the exception of $[(THF)Ca(NH_2BH_3)_2]_n$ (**I**, Figure 1b),[10] primary alkaline earth bis(amidotrihydroborates) [i.e., $Ae(NH_2BH_3)_2$] are typically unstable in solution, and their syntheses require heterogeneous or solid-state conditions.[13,14,20] Compound **I** has poor solubility and readily loses THF coordination under vacuum or in non-ethereal solvents, leading to polymeric or poorly-defined species. Employing more soluble secondary amine boranes, Hill and co-workers remarked that the formation of $Ae(NR_2BH_3)_2$ (R = alkyl, aryl) is complicated by incomplete aminolysis due to rapid catalytic dehydrogenation and/or dehydrocoupling reactions.[32,33] In the case for magnesium, the adduct $(THF)Mg(NMe_2BH_2NMe_2BH_3)_2$ (**II**) was isolated,[25] and the relevance of the complex $^-\{NMe_2BH_2NMe_2BH_3\}$ anion for catalytic dehydrogenation of $HNMe_2BH_3$ to $[Me_2NBH_2]_2$ has been further evaluated in molecular species based on d^0 metals.[23,24,26,34] Girolami has also reported a series of solution-stable alkaline earth bis(aminodiboranates) of the type $LAe(NMe_2(BH_3)_2)_2$ (**III**, Ae = Mg–Ba; L = Et_2O, THF, tmeda), although they were primarily investigated for chemical vapor deposition and not amine borane dehydrogenation.[35–38] However, these base-stabilized complexes are closer mimics of saline amidoboranes, and a more suitable choice of Lewis base may enhance their thermal stabilities for extensive molecular investigations.

Given our established interest in the stabilization of unusual organoalkaline earth complexes using carbene ligands,[39–46] we anticipated that the persistent coordination and stereoelectronic tunability of N-heterocyclic carbenes (NHCs) may enable the stabilization of structurally diverse magnesium amidoborane complexes for molecular studies. Notably, NHCs can modulate the nuclearity of magnesium hydride clusters based on ligand size, as our laboratory and others have discovered.[46–48] NHCs and cyclic (alkyl)(amino) carbenes (CAACs) are also active for the metal-free dehydropolymerization of amine boranes[49] and phosphine boranes,[50] with selective capture of dehydrogenation products (e.g., H_2, BH_2NR_2, $BH_2NR_2BH_3$) at the carbene C2 center. NHCs displayed significantly higher activity than common strong bases such as 4-dimethylaminopyridine (DMAP), phosphines, and N-heterocyclic olefins (NHOs) for the dynamic depolymerization of aminoboranes (Figure 1c).[51,52] Because these electronically flexible Lewis bases are, in their own right, active for amine borane dehydrocoupling reactions, the potential for non-innocent participation of NHCs in dehydrocoupling reactions involving magnesium amidoboranes is desirable for controlling amine borane dehydrogenation kinetics. We now report the syntheses, structural characterization, and spectroscopic studies of the first isolable, solution-stable magnesium bis(amidotrihydroborates) $[LMg(NR_2BH_3)_2]$, and further evaluate the influence of NHCs in aminoborane coupling in structurally diverse magnesium amidoboranes. A dynamic insertion/elimination of $Me_2N{=}BH_2$ was observed in the ^{NHC}C–Mg and Mg–N bonds of compounds containing the $^-\{NMe_2BH_2NMe_2BH_3\}$ anion, representing a rare example of reversible migratory insertion at a normal valent alkaline earth center. This fundamental organometallic process is unusual in the *s*-block,[53] and highlights the relevance of NHCs in understanding group 2 element-mediated amine borane dehydrocoupling.

Results and Discussion

Aminoborane Coupling at Carbene-Magnesium Centers

We have previously observed that 1,3-dialkyl-substituted NHCs are more suitable for the persistent stabilization of simple magnesium(II) complexes[42–44,54,55] than conventional diaryl-substituted NHCs, wherein destabilizing ligand dissociation is common due to steric complications.[56,57] Therefore, the ligand 1,3-diisopropyl-4,5-dimethylimidazol-2-ylidene (^{iPr}NHC)[58] was chosen for our investigations for its ease of synthesis and the availability of methine protons as a convenient spectroscopic handle. The reaction of $(^{iPr}NHC)Mg(N(SiMe_3)_2)_2$ (**1**)[46] and two equivalents of dimethylamine borane in hexanes afforded the triamide complex $(^{iPr}NHC–BN)Mg(NMe_2BH_3)(N(SiMe_3)_2)$ (**2**; ^{iPr}NHC–BN = ^{iPr}NHC–BH_2NMe_2) as a colorless crystalline solid in 67 % yield (Scheme 1). The ^{11}B NMR spectrum of **2** features two well-defined quartet ($\delta = -14.9$ ppm; $^1J_{BH} = 90.2$ Hz) and triplet ($\delta = -17.3$ ppm; $^1J_{BH} = 85.4$ Hz) resonances ascribed to the $-BH_3$ and $-BH_2$ groups respectively. The heteroleptic configuration of **2** is retained in solution, and no evidence of Schlenk rearrangements was observed in the ^{1}H NMR spectrum.

The molecular structure of **2** (Figure 2a) was unambiguously determined by single crystal X-ray diffraction,[59] which reveals a monomeric magnesium amidoborane complex in a trigonal planar central geometry (Σ N–Mg–N = 359.48°), albeit having Mg–HB agostic-type contacts from $^-NMe_2BH_3$ (Figure 2 caption). The B–N bond lengths are relatively similar in the neutral and anionic amidoborane ligands, which suggests charge delocalization in ^{iPr}NHC–BN. Hence, ^{iPr}NHC–BN may be considered a push-pull ligand (NHC→BN→Mg) similar to previous NHC-aminoborane adducts,[49,51] or a zwitterionic neutral donor (NHC–BN→Mg) in the coordination sphere of magnesium.

NMR-monitored stoichiometric reactions of **1** and $HNMe_2BH_3$ indicate the intermediacy of an $Mg(NMe_2BH_2NMe_2BH_3)$ unit ($\delta(BH_2)$ 2.53 ppm, $^1J_{BH} = 102.3$ Hz), as well as uncoordinated ^{iPr}NHC–BN ($\delta(BH_2)$ −13.4 ppm, $^1J_{BH} = 83.5$ Hz).[60] Therefore, in addition to

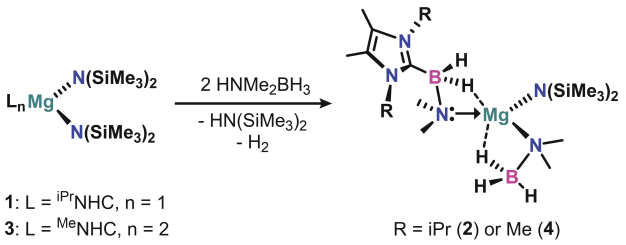

1: L = ^{iPr}NHC, n = 1
3: L = ^{Me}NHC, n = 2

R = iPr (**2**) or Me (**4**)

Scheme 1. Dimethylamine borane dehydrocoupling in the synthesis of a heteroleptic magnesium amidoborane complex.

© 2022 Wiley-VCH GmbH

15213773, 2022, 43, Downloaded from https://onlinelibrary.wiley.com/doi/10.1002/anie.202211496 by Mississippi State University, Wiley Online Library on [26/06/2023]. See the Terms and Conditions (https://onlinelibrary.wiley.com/terms-and-conditions) on Wiley Online Library for rules of use; OA articles are governed by the applicable Creative Commons License

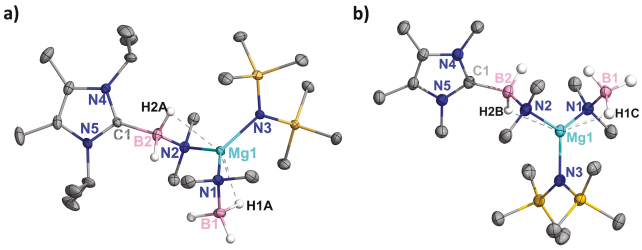

Figure 2. Molecular structures of **2** (a) and **4** (b). H atoms omitted for clarity, with the exception of B–H hydrides which were isotropically refined. Selected bond lengths (Å) and angles (°) for **2** [and **4**]: Mg1–N1, 2.0944(8) [2.088(3)]; Mg1–N2, 2.1301(8) [2.116(3)]; Mg1–N3, 1.9964(8) [1.990(3)]; Mg1–H1A, 2.095(14) [Mg1–H1C, 2.14 (4)]; Mg1–H2A, 2.373(13) [Mg1–H2B, 2.39(3)]; C1–B2, 1.6250(13) [1.625(5)]; B2–N2, 1.5653(13) [1.565(5)]; B1–N1, 1.5721(13) [1.560(5)]; N1–Mg1–N2, 131.96(3) [129.83(13)]; B2–N2–Mg1, 83.67(5) [90.1(2)]; H1A–Mg1–H2A, 147.3(5) [H1C–Mg1–H2B, 140.1(13)].

$Me_2N{=}BH_2$ capture at the ^{NHC}C–Mg bond in the formation of **2**, an NHC-mediated abstraction or migratory transfer of $Me_2N{=}BH_2$ from an $Mg(NMe_2BH_2NMe_2BH_3)$ unit cannot be discounted. In the absence of magnesium species, the reaction of ^{iPr}NHC and $HNMe_2BH_3$ yields the hydrogenated aminal ^{iPr}NHC-H_2, ^{iPr}NHC–BN and amino borane oligomers, which is consistent with previous reports of reactions between carbenes and secondary amine boranes.[49,50,61] However, in reactions of **1** and $HNMe_2BH_3$, ^{iPr}NHC-H_2 was only observed in minor quantities (ca. 6 %), suggesting that the NHC-coordination in **1** is persistent, and the observed dehydrocoupling processes are primarily metal-mediated.

In further attempts to isolate an $Mg(NMe_2BH_3)_2$ carbene complex, we posited that the electronic influence of multiple carbenes may discourage rapid dehydrocoupling reactions by weakening agostic β-BH interactions of the initial metathesis intermediate. Indeed, the coordination of multiple carbene ligands at divalent group 2 centers is known to modulate their electronic structures, even towards cationization in the absence of abstraction reagents.[43,44,62] While **1** does not react with an additional ^{iPr}NHC ligand due to steric complications, the reaction of $Mg(N(SiMe_3)_2)_2$ and the less hindered 1,3,4,5-tetramethylimidazol-2-ylidene (^{Me}NHC) affords $(^{Me}NHC)_2Mg(N(SiMe_3)_2)_2$ (**3**) as a colorless crystalline solid in 55 % yield. The subsequent reaction of **3** and $HNMe_2BH_3$ yielded a mixture of products including $(^{Me}NHC–BN)Mg(NMe_2BH_3)(N(SiMe_3)_2)$ (**4**) and uncoordinated ^{Me}NHC–BN due to the same dehydrocoupling processes observed in **1** (Scheme 1 and Figure S12). The molecular structure of **4** (Figure 2b) is structurally analogous to **2**, and their characteristic ^{11}B NMR resonances are nearly identical. Notwithstanding the unsuccessful isolation of a homoleptic $Mg(NMe_2BH_3)_2$ complex, these reactions highlight the facile nature of carbene-mediated $Me_2N{=}BH_2$ capture at magnesium. To elucidate the operative processes, the initial isolation of carbene-free $Mg(NMe_2BH_3)_2$ and $Mg(NMe_2BH_2NMe_2BH_3)_2$ species is necessary.

Synthesis of Homoleptic $Mg(NMe_2BH_3)_2$ Complexes

In addition to their thermal instability, the syntheses of $Mg(NH_2BH_3)_2$ salts require heterogeneous or solid-state reaction conditions (e.g., ball milling) due to the poor nucleophilicity of the typical magnesium hydride starting material (compared to CaH_2 and alkali metal hydrides).[14,17] In contrast to MgH_2, hydrocarbon-soluble magnesium alkyls and amides are highly reactive and prone to rapid dehydrocoupling.[25,32,33] In our initial attempts towards the selective isolation of $Mg(NMe_2BH_3)_2$, the reaction of Mg(nBu)$_2$ and two equivalents of $HNMe_2BH_3$ in hexanes at 0 °C yielded a viscous oil from which a few colorless crystals were obtained by mechanical agitation using a glass pipette. Spectroscopic analysis suggest the presence of multiple species, but only $Mg_4(\mu\text{-}O)(NMe_2BH_3)_6$ (**5**) was crystallographically identified (Figure 3a). Compound **5** presumably formed from the partial decomposition of $Mg(NMe_2BH_3)_2$ due to hydrolysis of trace moisture in the reaction solvent and suggests that the target bis(amidoborane) may further benefit from Lewis base stabilization. In the presence of THF, the adduct $(THF)_2Mg(NMe_2BH_3)_2$ (**6**) was obtained as a sticky solid, which was difficult to purify due to its extremely high solubility (Scheme 2). However, addition of the stronger base DMAP precipitated $(DMAP)_2$Mg-

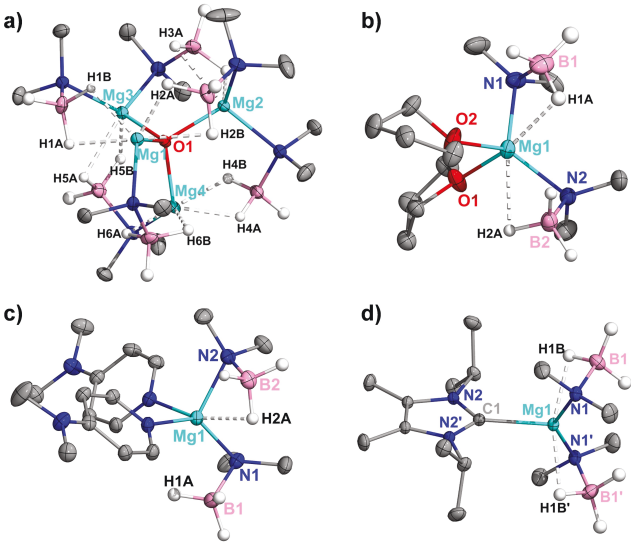

Figure 3. Molecular structures of **5** (a), **6** (b), **7** (c) and **8** (d). H atoms are omitted for clarity, with the exception of B–H hydrides which were isotropically refined. Selected bond lengths (Å) and angles (°): **5**: Mg1–H1B, 1.975(15); Mg1–H2A, 1.949(17); Mg1–H1A, 2.132(16); Mg1–H2B, 2.254(17); Mg2–H3B, 1.960(17); Mg1–O1, 1.9718(9); Mg2–O1, 2.132(16); Mg1–N6, 2.0873(11); Mg1–O1–Mg2, 107.45(4); H3A–Mg2–H3B, 52.1(6); H1A–Mg1–H2B, 173.9(6). **6**: Mg1–N1, 2.1034(15); Mg1–H1A, 2.16(2); Mg1–H2A, 2.353(19); B1–N1, 1.578(2); N1–Mg1–N1′, 113.79(6). **7**: Mg1–N1, 2.1099(14); Mg1–N2, 2.1147(14); Mg1–H2A, 2.210(18); Mg1···H1A, 2.477(21); B1–N1, 1.563(2); B2–N2, 1.581(2); N1–Mg1–N1′, 113.18(6). **8**: Mg1–C1, 2.2062(10); Mg1–N1, 2.0848(7); Mg1–H1B, 2.104(13); B1–N1, 1.5707 (11); N1–Mg1–N′, 143.23(4); H1B–Mg1–H1B′, 161.82(3). Symmetry transformations used to generate equivalent atoms (A′) in **8**: $-x+1$, y, $-z+1/2$.

© 2022 Wiley-VCH GmbH

15213773, 2022, 43, Downloaded from https://onlinelibrary.wiley.com/doi/10.1002/anie.202211496 by Mississippi State University, Wiley Online Library on [26/06/2023]. See the Terms and Conditions (https://onlinelibrary.wiley.com/terms-and-conditions) on Wiley Online Library for rules of use; OA articles are governed by the applicable Creative Commons License

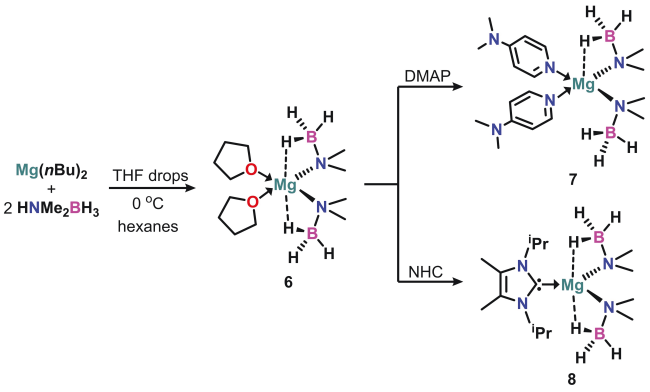

Scheme 2. Dimethylamine borane dehydrocoupling in the synthesis of a heteroleptic magnesium amidoborane complex.

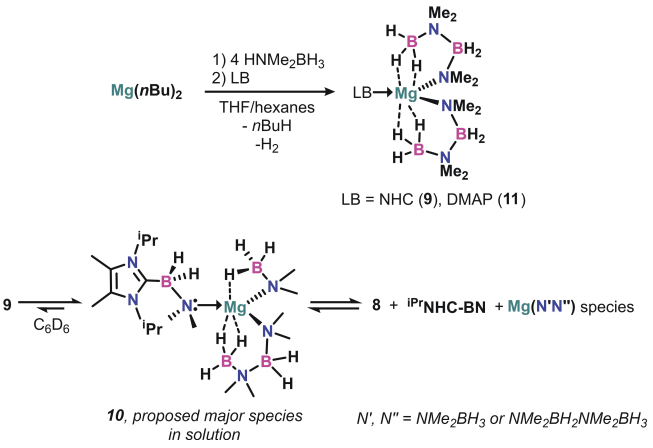

Scheme 3. Carbene-mediated shuttling of $Me_2N{=}BH_2$ in an Mg-$(NMe_2BH_2NMe_2BH_3)_2$ complex.

$(NMe_2BH_3)_2$ (**7**) as a free-flowing white solid, which is easily purified by a hexanes or toluene wash. Likewise, in situ NHC complexation to **6** afforded (^{iPr}NHC)Mg$(NMe_2BH_3)_2$ (**8**) as a colorless crystalline solid in 74 % yield (Scheme 2). In contrast to the case for **5** and **6**, the identity and purity of **7** and **8** were also confirmed by heteronuclear (^{1}H, ^{11}B, ^{13}C) NMR spectroscopy.

In contrast to the extensive network of multinuclear Mg···HB interactions in **5** and polymeric Mg$(NH_2BH_3)_2$ complexes,[16,17] Lewis base coordination in **6**, **7**, and **8** resulted in monomeric complexes (Figures 3b–d). The shortest Mg–H contacts in **6** (2.16(2) and 2.353(19) Å) and **7** (2.210(18) Å) are elongated from those of **8** (both 2.104 (13) Å). The ^{NHC}C–Mg bond in **8** (2.2062(10) Å) is comparable to the same for **1** and similar tricoordinate magnesium amides stabilized by ^{iPr}NHC (2.205(6)–2.2120(19) Å).[46,54] Hence, the carbene coordination is expected to be persistent in solution. In the solid state, **7** and **8** are indefinitely stable in inert atmosphere under ambient conditions, and no decomposition was spectroscopically observed in their anhydrous benzene solutions over several weeks. Thus, the benefit of Lewis base stabilization of magnesium amidotrihydroborates for solution-state investigations is evident.

Dynamic Aminoborane Coupling in Complexes Containing the $^-${$NMe_2BH_2NMe_2BH_3$} Anion

The reaction of Mg(nBu)$_2$ and four equivalents of $HNMe_2BH_3$, followed by NHC complexation affords (^{iPr}NHC)Mg$(NMe_2BH_2NMe_2BH_3)_2$ (**9**) as a colorless crystalline solid (Scheme 3).[AO1] The molecular structure of **9** is analogous to the THF adduct (**II**)[25] as a monomeric compound with four agostic Mg···HB contacts (Figure 4a). The ^{NHC}C–Mg bond in **9** (2.3450(16) Å) is significantly longer than that of **8** (2.2062(10) Å), and to the best of our knowledge, the longest known ^{carbene}C–Mg^{II} bond in the literature. Indeed, it closely compares with ^{carbene}C–Mg^{I} systems (2.312(3)–2.341(2) Å),[63] whose elongated bonds are owed to the increased ionic radii of Mg^{I}. Similar to **II**, there are pronounced disparities in the B–N bond lengths in **9** (Δ 0.024–0.051 Å) which suggests differing charge localization in the $^-${$NMe_2BH_2NMe_2BH_3$} anion.

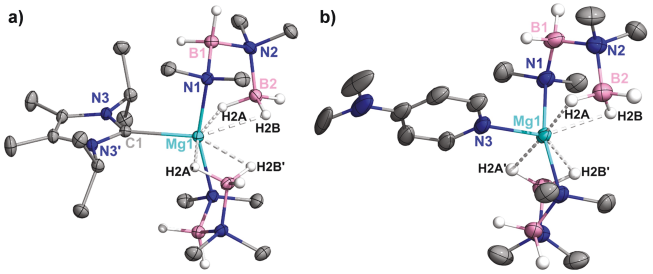

Figure 4. Molecular structures of **9** (a) and **11** (b). H atoms omitted for clarity, with the exception of B–H hydrides which were isotropically refined. Selected bond lengths (Å) and angles (°) in **9** [and **11**]: Mg1–C1, 2.3450(16) [Mg1–N3, 2.144(3)]; Mg1–N1, 2.1663(9) [2.1679 (18)]; Mg1–H2 A, 2.107(14) [2.18(3)]; Mg1–H2B, 2.295(15) [2.21(3)]; B1–N1, 1.5607(16) [1.547(4)]; B1–N2, 1.6115(16) [1.618(4)]; B2–N2, 1.5846(16) [1.580(3)]; N1–Mg1–N1′, 159.51(6) [163.16(12)]. Symmetry transformations used to generate equivalent atoms (A′) in **9** [and **11**]: $-x+1, y, -z+1/2$ [$-x+1, y, -z+3/2$].

Despite crystallographic confirmation, **9** is unobserved by NMR but undergoes dynamic disproportionation in solution (C_6D_6) to several products including **8**, **^{iPr}NHC–BN**, and a primary product presumed to be (^{iPr}NHC–BN)Mg$(NMe_2BH_3)(NMe_2BH_2NMe_2BH_3)$ (**10**). Efforts to unambiguously identify **10** by X-ray crystallography only led to the isolation of **8**, **9**, or **^{iPr}NHC–BN**, depending on solvent or temperature conditions. However, the assignment of **10** is based on several spectroscopic observations. The carbene methine protons in **10** ($\delta_H = 4.89$ ppm) are downfield from **8** ($\delta_H = 4.57$ ppm), which suggests ^{iPr}NHC coordination to a more Lewis acidic fragment such as a borane, in contrast to the donor-rich environment of **9**. In the ^{11}B NMR spectrum, a prominent Mg$(NMe_2BH_2NMe_2BH_3)$ resonance (t, $\delta =$ 2.89 ppm, $^1J_{BH}$ 101.8 Hz) was observed, but resonances due to Mg(NMe_2BH_3) and ^{iPr}NHC–BN units were overlapped. In variable temperature (VT) ^{1}H NMR studies, the methine resonance for **10** decoalesced to two broad resonances at

© 2022 Wiley-VCH GmbH

15213773, 2022, 43, Downloaded from https://onlinelibrary.wiley.com/doi/10.1002/anie.202211496 by Mississippi State University, Wiley Online Library on [26/06/2023]. See the Terms and Conditions (https://onlinelibrary.wiley.com/terms-and-conditions) on Wiley Online Library for rules of use; OA articles are governed by the applicable Creative Commons License

−55 °C (Figure S22), likely due to the heteroleptic nature of the proposed structure. Free NHC was also observed below −30 °C, which supports the likelihood of NHC dissociation and abstraction of aminoborane from Mg(NMe$_2$BH$_2$NMe$_2$BH$_3$). At higher temperatures (25–100 °C), the increased formation of **8** and **^{iPr}NHC–BN** and concomitant decrease in **10** was observed (Figure S23). Nuclear Overhauser effect spectroscopy (NOESY) confirmed direct chemical exchange between **8**, **^{iPr}NHC–BN** and **10**, and in the latter, through-space interactions between the carbene methine protons and borane hydrides support the presence of an ^{iPr}NHC–BN coordination adduct (Figure S27). Furthermore, we probed the relative molecular masses of the species in solution through diffusion ordered spectroscopy (DOSY) experiments, and the smallest diffusion coefficient was observed for **10**, which is expectedly the heaviest molecule.

Given the relative stability of **II**, it is clear that the dynamic disproportionation of **9** via aminoborane migration is carbene-mediated. The thermodynamic impetus for disproportionation seems to be the formation of a stable ^{iPr}NHC–BN unit, and the kinetic production of **8** is likely driven by presence of Lewis acidic magnesium species due to ^{iPr}NHC–BN dissociation and subsequent base substitution reactions from the borane (Me$_2$N=BH$_2$) to the base-free magnesium species (Scheme 4). Manners previously realized that NHC–BH$_2$NRR′ complexes, stabilized by 1,3-diaryl-substituted NHCs, are labile via spontaneous dissociation in solution or carbene transfer to Lewis acids (e.g. B(C$_6$F$_5$)$_3$).[51] In the case for **^{iPr}NHC–BN**, no dynamic dissociation was observed at variable temperatures (203–353 K), but substitution reactions with B(C$_6$F$_5$)$_3$ or Mg(HMDS)$_2$ was facile (Figure S7). Strong bases such as DMAP and triphenylphosphine do not form adducts with Me$_2$N=BH$_2$ in their reactions with **II** or [Me$_2$N–BH$_2$]$_2$. Notably, (DMAP)Mg(NMe$_2$BH$_2$NMe$_2$BH$_3$)$_2$ (**11**) was subsequently isolated (Scheme 3 and Figure 4b), and no dynamic processes were observed in solution.

The impact of Lewis acidic magnesium species in the dynamic disproportionation of **9** was further evaluated in substitution reactions with Lewis bases. The ^{1}H NMR spectrum of **9** in THF-d_8 revealed only one set of carbenic resonances due to uncoordinated ^{iPr}NHC–BN, whereas the magnesium species are solvated. Additionally, the reaction of **9** and two equivalents of ^{iPr}NHC enabled complete abstraction of Me$_2$N=BH$_2$ from Mg(NMe$_2$BH$_2$NMe$_2$BH$_3$) units to yield **8** and **^{iPr}NHC–BN** (Figure 5), and quench dynamic exchange processes. The persistence of **8** instead of (^{iPr}NHC–BN)-Mg adducts suggest that ^{iPr}NHC–BN is a weaker base than NHCs for the stabilization of magnesium bis(amidoboranes), although it may serve as a mediator for aminoborane migration. Importantly, these observations suggest competitive Lewis acidities between Me$_2$N=BH$_2$ and base-free magnesium amidoboranes, which may promote dynamic acid/base exchange processes as described in Scheme 4, reaction B.

In these reactions, it is reasonable to expect Me$_2$N=BH$_2$ abstraction by the direct action of NHCs on Mg(NMe$_2$BH$_2$NMe$_2$BH$_3$) units (Scheme 4, reaction D). However, the likelihood of varied charge localization in $^-${NMe$_2$BH$_2$NMe$_2$BH$_3$} supports spontaneous Me$_2$N=BH$_2$ elimination. The complex anion may be regarded as a donor-acceptor ($^-$NMe$_2$BH$_2$NMe$_2$)(BH$_3$) adduct wherein BH$_3$ may be supported by either nitrogen base,[28,64] which permits the formation of ($^-$NMe$_2$BH$_3$) and Me$_2$N=BH$_2$. In addition, β- and δ-BH elimination processes from

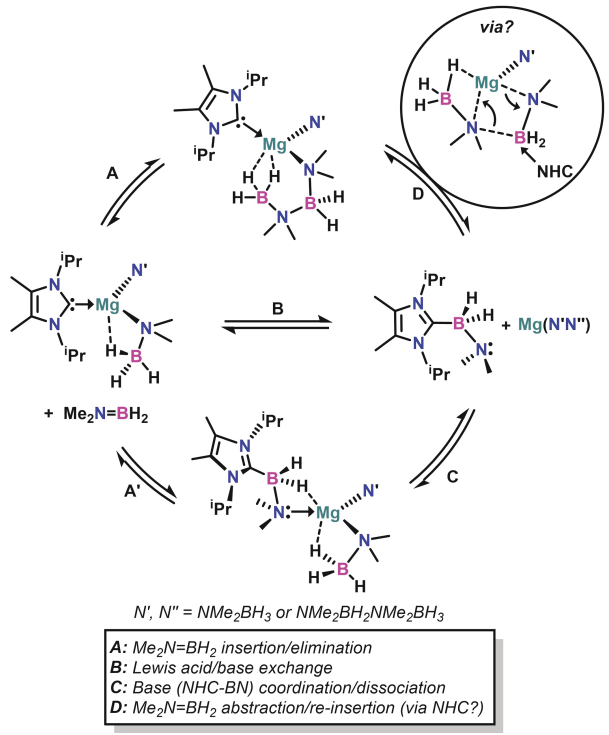

Scheme 4. Proposed mechanism for the disproportionation of carbene-stabilized RMg(NMe$_2$BH$_2$NMe$_2$BH$_3$) complexes.

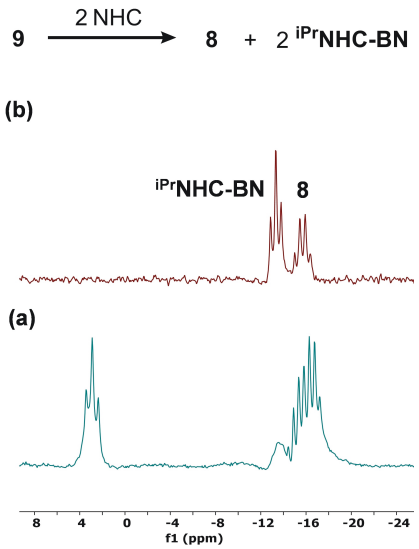

Figure 5. Stack plot of ^{11}B NMR spectra showing the presence of multiple species in **9** (a, bottom), and disappearance of Mg(NMe$_2$*BH$_2$*NMe$_2$BH$_3$) units upon reaction with two equivalents of ^{iPr}NHC (b, top).

© 2022 Wiley-VCH GmbH

15213773, 2022, 43, Downloaded from https://onlinelibrary.wiley.com/doi/10.1002/anie.202211496 by Mississippi State University, Wiley Online Library on [26/06/2023]. See the Terms and Conditions (https://onlinelibrary.wiley.com/terms-and-conditions) on Wiley Online Library for rules of use; OA articles are governed by the applicable Creative Commons License

$^{-}\{NMe_2BH_2NMe_2BH_3\}$ should be considered. The former yields $HB(NMe_2)_2$ and BH_3 or BH_4^-, which were not detected in **9** even at elevated temperatures, and the latter yields cyclic tetramethylborazane ($[Me_2N–BH_2]_2$; t, 5.66 ppm, $^1J_{BH}$ 107.5 Hz), which was only observed above 100 °C in the VT ^{11}B NMR experiments, or partially accumulated during the sustained decomposition of **9** (65 °C, 16 h). However, the production of monomeric $Me_2N{=}BH_2$ is important to the dynamic processes because ^{iPr}NHC readily captures $Me_2N{=}BH_2$ at room temperature, but requires elevated temperatures (80 °C) to split the $[Me_2N–BH_2]_2$ dimer. Furthermore, metal hydride species due to unassisted β- or δ-BH elimination processes were not observed. A β-BH elimination in **8** should also yield $Me_2N{=}BH_2$, but this process is discounted by the compound's thermal stability in refluxing benzene (85 °C, 24 h) with no spectroscopic evidence of decomposition. Indeed, unassisted β- or δ-BH elimination from magnesium amidoboranes are known to be high energy processes,[26] and unlikely to be predominant in the disproportionation of **9**.

In further efforts to elucidate some of the unobserved intermediates described in Scheme 4, we investigated the reaction of **8** and $HNMe_2BH_3$, which yielded (^{iPr}NHC)Mg(NMe_2BH_3)($NMe_2BH_2NMe_2BH_3$) (**12**) as a colorless crystalline solid (Scheme 5 and Figure 6). Owing to close Mg–H contacts from $^{-}\{NMe_2BH_2NMe_2BH_3\}$, the ^{NHC}C–Mg bond in **12** (2.2287(15) Å) is slightly elongated from **8** (2.2062 (10) Å), and the geometry around the magnesium atom is modestly distorted from trigonal planar (sum of metal-ligand angles 354.9°). In contrast to **9** and **11**, the B–N bond lengths within $\{NMe_2BH_2NMe_2BH_3\}$ in **12** are equivalent within standard deviation.

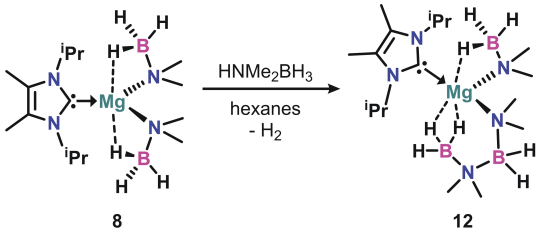

Scheme 5. Isolation of (^{iPr}NHC)Mg(NMe_2BH_3)($NMe_2BH_2NMe_2BH_3$) (**12**).

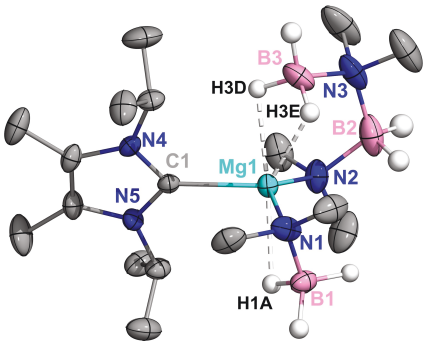

Figure 6. Molecular structure of **12**. H atoms are omitted for clarity, with the exception of B–H hydrides which were isotropically refined. Selected bond lengths (Å) and angles (°): Mg1–C1, 2.2287(15); Mg1–N1, 2.0843(14); Mg1–N2, 2.1328(14); Mg1–H1A, 2.20(2); Mg1–H3D, 2.222(19); Mg1–H3E, 2.09(2); B1–N1, 1.512(3); B2–N2, 1.581(3); B3–N3, 1.574(3); N1–Mg1–C1, 107.28(6); N1–Mg1–N2, 132.89(7); H1A–Mg1–H3D, 168.4(7).

The isolation of **12** in the solid-state instead of (^{iPr}NHC–BN)Mg(NMe_2BH_3)$_2$ contrasts the observed $Me_2N{=}BH_2$ capture at the ^{NHC}C–Mg bond in the formation of **2** and indicates that small changes in the metal coordination environment [$N(SiMe_3)_2$ vs NMe_2BH_3] can substantially influence the nature of the thermodynamic product. As anticipated, **12** was not observed in solution, but is prone to the same dynamic processes observed for **9** (Scheme 4). Due to the heteroleptic nature of **12**, initial Schlenk type rearrangements in solution towards **8** and **9** cannot be discounted. Comparative dehydrocoupling reactions of **2** and $HNMe_2BH_3$ yielded (^{iPr}NHC–BN)Mg($N(SiMe_3)_2$)($NMe_2BH_2NMe_2BH_3$) (**13**), and spectroscopic studies indicate disproportionation to **2**, **8**, **10**, and **^{iPr}NHC–BN**, which likely involves Schlenk rearrangements (Figure S37).

Computational Studies

In order to gain additional insight into the aminoborane migratory coupling processes, density functional theory computations were performed at the ωB97X-D/cc-PVDZ level of theory.[65–70] To minimize complications due to multiple metal-hydride interactions, only one amidoborane unit at the magnesium center was considered. Therefore, the conversion of **1** to **2** and **min-V** was selected as an appropriate thermodynamic model for the dehydrocoupling and migratory insertion processes (Figure 7). The corresponding electronic energies are described in Figure S44.

The metathetical reaction of **1** and $HNMe_2BH_3$ to form the mono-amidoborane (**int-1**) is exergonic by 8.2 kcal mol^{-1}. Subsequent amine borane dehydrogenation is anticipated to proceed via β-BH elimination processes that are unassisted (path A, black) or amine borane-assisted (path B, blue). In path A, an initial amidoborane rearrangement cleaves the Mg–N bond via **TS-2** in favor of hydride contacts in **int-2**. A formal hydride transfer to Mg incurs a +13.0 kcal mol^{-1} penalty in **TS-3**, but the resultant aminoborane remains coordinated to the metal center via BH contacts in **int-3**. The addition of a second $HNMe_2BH_3$ unit to **int-3** results in an [Mg]-H-H-NMe_2BH_3 species (**int-4**), which releases molecular H_2 towards the separated species LMg(NR′)(NMe_2BH_3) + $Me_2N{=}BH_2$ (**int-5**).

Comparable unassisted β-hydride elimination has also been modelled in β-diketiminate magnesium systems,[71] and this mechanism is broadly accepted for rationalizing amine borane dehydrogenation at group 2 centers.[5] However, recent studies have reconsidered the likelihood of this process.[26] The anticipated metal-hydride intermediates were not observed in thermal studies of magnesium amidoboranes, and only identified in the presence of additional equivalents of amine borane. Therefore, an amine borane-assisted β-hydride elimination and dehydrocoupling rationale is increasingly adopted.[23,26] Path B (blue) provides

© 2022 Wiley-VCH GmbH

15213773, 2022, 43, Downloaded from https://onlinelibrary.wiley.com/doi/10.1002/anie.202211496 by Mississippi State University, Wiley Online Library on [26/06/2023]. See the Terms and Conditions (https://onlinelibrary.wiley.com/terms-and-conditions) on Wiley Online Library for rules of use; OA articles are governed by the applicable Creative Commons License

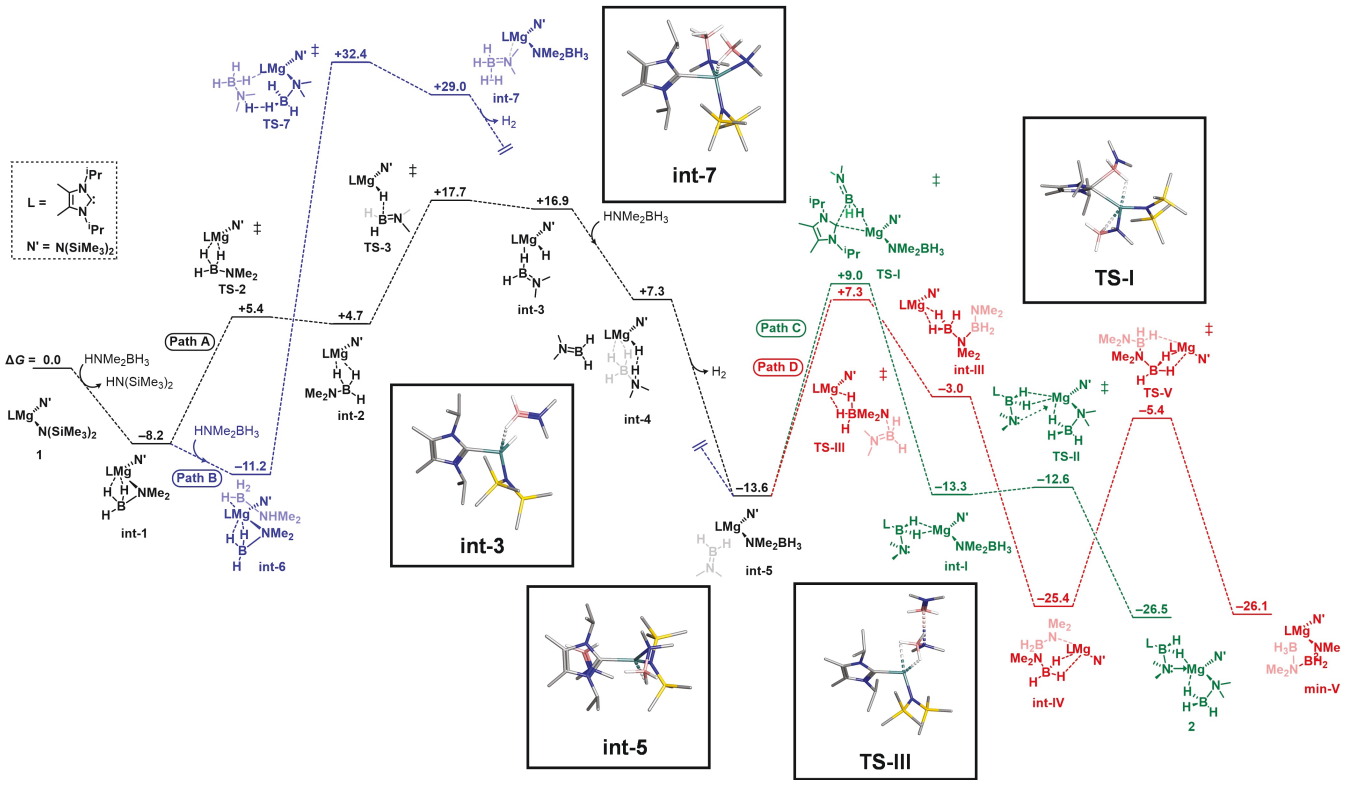

Figure 7. Calculated relative free energies (ΔG, kcal mol^{-1}) for the dehydrocoupling of **1** to **2** at the ωB97X-D/cc-PVDZ level of theory. Different models for H_2 elimination [path A (black) and path B (blue)] and $Me_2N{=}BH_2$ migratory coupling [path C (green) and path D (red)] were considered.

a possible model for this process, beginning with an exergonic (−3.0 kcal mol^{-1}) coordination of $HNMe_2BH_3$ to the Mg center in **int-1** via hydride contacts (**int-6**). The interaction of amine proton and amidoborane hydride in **int-6** proceeds through a high energy transition state (**TS-7**, $\Delta\Delta G^{\ddagger} = +43.6$ kcal mol^{-1}), resulting in **int-7**, which involves a loosely bound metal-aminoborane species with a σ-bound H_2 unit. Entropic release of molecular H_2 towards **int-5** ($\Delta\Delta G = -42.6$ kcal mol^{-1}) is the thermodynamic driving force for this pathway, but the rate determining step (**TS-7**) suggests that it is less feasible than path A.

Following dehydrogenation, $Me_2N{=}BH_2$ coupling into the ^{NHC}C–Mg (path C, green) or Mg–N bond (path D, red) involves relatively low transformation energies. In path C, NHC migration from Mg to $Me_2N{=}BH_2$ (via **TS-I**, $\Delta\Delta G^{\ddagger} = +22.6$ kcal mol^{-1}) forms a hydride-stabilized intermediate **int-I**. The formation of **2** through amide (:NMe_2–BH_2L) coordination to the Mg center is facile due to the low-lying nature of **TS-II** ($\Delta\Delta G^{\ddagger} = +0.7$ kcal mol^{-1}). Notably, the free energy of dissociation of **2** into free **^{iPr}NHC–BN** and $Mg(N(SiMe_3)_2)(NMe_2BH_3)$ is +24.1 kcal mol^{-1} (Figure S43). In path D, the initial step (**TS-III**, +20.9 kcal mol^{-1}) is comparable in energy to **TS-I** in path C and involves acid-base complexation of aminoborane and amidoborane to form **int-III**. In the latter, the $^{-}${$NMe_2BH_2NMe_2BH_3$} anion is solely coordinated to Mg via BH_3, but subsequent amide coordination stabilizes the metal center to form **int-IV**. The local minimum **min-V** is structurally and thermodynamically comparable to **int-IV**, and results from further amide dissociation and rearrangement via **TS-V**. Although **min-V** was not observed in the solid state, there is ^{11}B NMR evidence for the rapid formation of the $^{-}${$NMe_2BH_2NMe_2BH_3$} anion in the reaction of **1** and $HNMe_2BH_3$. The isolation of **12** also corroborates the accessibility of this pathway. Therefore, the low transformation energies between stationary points in paths C and D suggest that the thermal migratory coupling of $Me_2N{=}BH_2$ is feasible.

Compared to **min-V**, **2** is thermodynamically favored by 0.4 kcal mol^{-1}. In contrast to **9** and **12** however, no dynamic aminoborane migration was experimentally observed for **2**. The facility of these processes for **9** and **12** may be due to the abundance of amidoborane units in their coordination sphere, whereby aminoborane coupling/decoupling results in bis(amidoborane) species capable of the same processes (i.e., **8** and **10**). Increased metal-hydride contacts in these bis(amidoborane) complexes may further stabilize their transition states for more facile transformations. The prevalence of stabilizing hydride contacts throughout the proposed mechanism is highlighted in selected stationary points in Figure S45. Indeed, the relative thermodynamic energies of **8**–**12** are partially correlated with the number of metal-hydride contacts and are in the order of **9** < **10** < **12** < **8** (Figure 8). Additionally, Wiberg bond indices (WBI) and Mayer bond orders (MBO) support dissimilar N–B bond orders for the $^{-}${$NMe_2BH_2NMe_2BH_3$} anion (Table S5), as

© 2022 Wiley-VCH GmbH

15213773, 2022, 43, Downloaded from https://onlinelibrary.wiley.com/doi/10.1002/anie.202211496 by Mississippi State University, Wiley Online Library on [26/06/2023]. See the Terms and Conditions (https://onlinelibrary.wiley.com/terms-and-conditions) on Wiley Online Library for rules of use; OA articles are governed by the applicable Creative Commons License

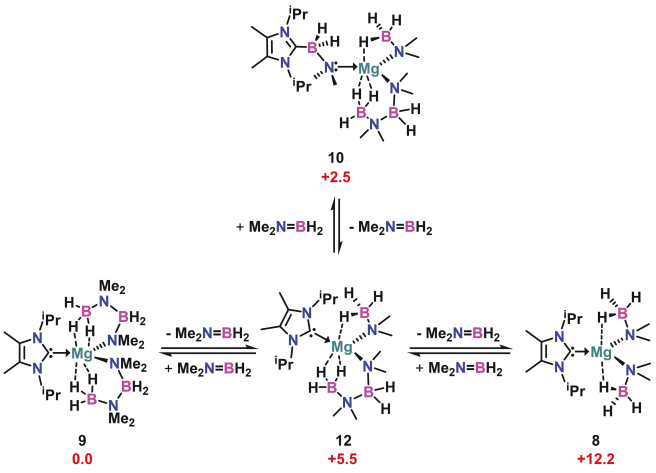

Figure 8. Relative free energies (ΔG, kcal mol^{-1}) of aminoborane insertion/elimination between compounds **8**, **9**, **10**, and **12**.

well as indicate significant bonding interactions between magnesium and amidoborane boron atoms (Table S4).

Conclusion

The dynamic migration of aminoborane units in the coordination sphere of magnesium has been investigated. It was determined that these dynamic processes are motivated by: (i) Variable charge localization within $^{-}\{NMe_2BH_2NMe_2BH_3\}$, which results in the spontaneous elimination of $Me_2N{=}BH_2$; (ii) Facile capture of $Me_2N{=}BH_2$ by NHC ligands, and thermodynamic stability of the subsequent ^{iPr}NHC–BN unit; (iii) Availability of base-free, Lewis acidic $RMg(NMe_2BH_3)$ units for an initial acid-base exchange with ^{iPr}NHC–BN to release $Me_2N{=}BH_2$, followed by aminoborane re-insertion into the Mg–N bond. These processes are reminiscent of reversible 1,2-migratory insertion of unsaturated 2e$^-$ ligands in transition metal chemistry, and to the best of our knowledge, unobserved in normal valent *s*-block element chemistry. Specifically, such NHC-mediated shuttling of aminoboranes at magnesium is anticipated to have significant implications for the development of reversible hydrogen storage materials based on magnesium amidoboranes.

Acknowledgements

The authors acknowledge the David and Lucile Packard Foundation and the National Science Foundation Major Research Instrumentation (CHE-2018870, R.J.G.) and Chemical Catalysis (CHE-2102552, C.E.W.) programs for support of this work. A.D.O. thanks the Jefferson Scholars Foundation for a Burn Family Melville Foundation Graduate Fellowship. N.C.F. acknowledges the National Science Foundation for a Graduate Research Fellowship (Grant #1842490). We also thank Dr. Jeff Elena (University of Virginia) for assistance with 2D NMR experiments.

Conflict of Interest

The authors declare no conflict of interest.

Data Availability Statement

The data that support the findings of this study are available in the supplementary material of this article.

Keywords: Amine Borane · Carbenes · Hydrogen Storage · Magnesium · Migratory Insertion

[1] A. Rossin, M. Peruzzini, *Chem. Rev.* **2016**, *116*, 8848–8872.
[2] R. Kumar, A. Karkamkar, M. Bowden, T. Autrey, *Chem. Soc. Rev.* **2019**, *48*, 5350–5380.
[3] J. Graetz, *Chem. Soc. Rev.* **2009**, *38*, 73–82.
[4] T. B. Marder, *Angew. Chem. Int. Ed.* **2007**, *46*, 8116–8118; *Angew. Chem.* **2007**, *119*, 8262–8264.
[5] T. E. Stennett, S. Harder, *Chem. Soc. Rev.* **2016**, *45*, 1112–1128.
[6] C. W. Hamilton, R. T. Baker, A. Staubitz, I. Manners, *Chem. Soc. Rev.* **2009**, *38*, 279–293.
[7] Y. S. Chua, P. Chen, G. Wu, Z. Xiong, *Chem. Commun.* **2011**, *47*, 5116–5129.
[8] A. Karkamkar, C. Aardahl, T. Autrey, *Mater. Matters* **2007**, *2*, 6–9.
[9] N. C. Smythe, J. C. Gordon, *Eur. J. Inorg. Chem.* **2010**, 509–521.
[10] H. V. K. Diyabalanage, R. P. Shrestha, T. A. Semelsberger, B. L. Scott, M. E. Bowden, B. L. Davis, A. K. Burrell, *Angew. Chem. Int. Ed.* **2007**, *46*, 8995–8997; *Angew. Chem.* **2007**, *119*, 9153–9155.
[11] H. V. K. Diyabalanage, T. Nakagawa, R. P. Shrestha, T. A. Semelsberger, B. L. Davis, B. L. Scott, A. K. Burrell, W. I. F. David, K. R. Ryan, M. O. Jones, P. P. Edwards, *J. Am. Chem. Soc.* **2010**, *132*, 11836–11837.
[12] Z. Xiong, C. K. Yong, G. Wu, P. Chen, W. Shaw, A. Karkamkar, T. Autrey, M. O. Jones, S. R. Johnson, P. P. Edwards, W. I. F. David, *Nat. Mater.* **2008**, *7*, 138–141.
[13] Q. Zhang, C. Tang, C. Fang, F. Fang, D. Sun, L. Ouyang, M. Zhu, *J. Phys. Chem. C* **2010**, *114*, 1709–1714.
[14] J. Luo, X. Kang, P. Wang, *Energy Environ. Sci.* **2013**, *6*, 1018–1025.
[15] H. Wu, W. Zhou, T. Yildirim, *J. Am. Chem. Soc.* **2008**, *130*, 14834–14839.
[16] Y. S. Chua, G. Wu, Z. Xiong, A. Karkamkar, J. Guo, M. Jian, M. W. Wong, T. Autrey, P. Chen, *Chem. Commun.* **2010**, *46*, 5752–5754.
[17] X. Kang, H. Wu, J. Luo, W. Zhou, P. Wang, *J. Mater. Chem.* **2012**, *22*, 13174–13179.
[18] H. Wu, W. Zhou, F. E. Pinkerton, M. S. Meyer, Q. Yao, S. Gadipelli, T. J. Udovic, T. Yildirim, J. J. Rush, *Chem. Commun.* **2011**, *47*, 4102–4104.
[19] Y. S. Chua, W. Li, G. Wu, Z. Xiong, P. Chen, *Chem. Mater.* **2012**, *24*, 3574–3581.
[20] Y. S. Chua, H. Wu, W. Zhou, T. J. Udovic, G. Wu, Z. Xiong, M. W. Wong, P. Chen, *Inorg. Chem.* **2012**, *51*, 1599–1603.
[21] R. Nolla-Saltiel, A. M. Geer, W. Lewis, A. J. Blake, D. L. Kays, *Chem. Commun.* **2018**, *54*, 1825–1828.
[22] A. C. A. Ried, L. J. Taylor, A. M. Geer, H. E. L. Williams, W. Lewis, A. J. Blake, D. L. Kays, *Chem. Eur. J.* **2019**, *25*, 6840–6846.
[23] L. Wirtz, W. Haider, V. Huch, M. Zimmer, A. Schäfer, *Chem. Eur. J.* **2020**, *26*, 6176–6184.

© 2022 Wiley-VCH GmbH

15213773, 2022, 43, Downloaded from https://onlinelibrary.wiley.com/doi/10.1002/anie.202211496 by Mississippi State University, Wiley Online Library on [26/06/2023]. See the Terms and Conditions (https://onlinelibrary.wiley.com/terms-and-conditions) on Wiley Online Library for rules of use; OA articles are governed by the applicable Creative Commons License

[24] P. Bellham, M. S. Hill, G. Kociok-Köhn, *Dalton Trans.* **2015**, *44*, 12078–12081.
[25] D. J. Liptrot, M. S. Hill, M. F. Mahon, D. J. MacDougall, *Chem. Eur. J.* **2010**, *16*, 8508–8515.
[26] P. Bellham, M. D. Anker, M. S. Hill, G. Kociok-Köhn, M. F. Mahon, *Dalton Trans.* **2016**, *45*, 13969–13978.
[27] C. Jones, S. J. Bonyhady, S. Nembenna, A. Stasch, *Eur. J. Inorg. Chem.* **2012**, 2596–2601.
[28] J. Spielmann, S. Harder, *J. Am. Chem. Soc.* **2009**, *131*, 5064–5065.
[29] J. Spielmann, G. Jansen, H. Bandmann, S. Harder, *Angew. Chem. Int. Ed.* **2008**, *47*, 6290–6295; *Angew. Chem.* **2008**, *120*, 6386–6391.
[30] J. Spielmann, D. F. J. Piesik, S. Harder, *Chem. Eur. J.* **2010**, *16*, 8307–8318.
[31] J. Spielmann, M. Bolte, S. Harder, *Chem. Commun.* **2009**, 6934–6936.
[32] M. S. Hill, M. Hodgson, D. J. Liptrot, M. F. Mahon, *Dalton Trans.* **2011**, *40*, 7783–7790.
[33] P. Bellham, M. S. Hill, G. Kociok-Köhn, D. J. Liptrot, *Dalton Trans.* **2013**, *42*, 737–745.
[34] M. S. Hill, G. Kociok-Köhn, T. P. Robinson, *Chem. Commun.* **2010**, *46*, 7587–7589.
[35] S. R. Daly, B. J. Bellott, M. A. Nesbit, G. S. Girolami, *Inorg. Chem.* **2012**, *51*, 6449–6459.
[36] A. C. Dunbar, G. S. Girolami, *Inorg. Chem.* **2014**, *53*, 888–896.
[37] A. C. Dunbar, R. Joseph Lastowski, G. S. Girolami, *Inorg. Chem.* **2020**, *59*, 16893–16904.
[38] D. Y. Kim, G. S. Girolami, *Inorg. Chem.* **2010**, *49*, 4942–4948.
[39] G. Wang, J. E. Walley, D. A. Dickie, S. Pan, G. Frenking, R. J. Gilliard, *J. Am. Chem. Soc.* **2020**, *142*, 4560–4564.
[40] G. Wang, J. Walley, D. Dickie, A. Molino, D. Wilson, R. J. Gilliard, *Angew. Chem. Int. Ed.* **2021**, *60*, 9407–9411; *Angew. Chem.* **2021**, *133*, 9493–9497.
[41] L. A. Freeman, J. E. Walley, A. D. Obi, G. Wang, D. A. Dickie, A. Molino, D. J. D. Wilson, R. J. Gilliard, *Inorg. Chem.* **2019**, *58*, 10554–10568.
[42] Y. O. Wong, L. A. Freeman, A. D. Agakidou, D. A. Dickie, C. E. Webster, R. J. Gilliard, *Organometallics* **2019**, *38*, 688–696.
[43] A. D. Obi, J. E. Walley, N. C. Frey, Y. O. Wong, D. A. Dickie, C. E. Webster, R. J. Gilliard, *Organometallics* **2020**, *39*, 4329–4339.
[44] A. D. Obi, H. R. Machost, D. A. Dickie, R. J. Gilliard, *Inorg. Chem.* **2021**, *60*, 12481–12488.
[45] J. E. Walley, A. D. Obi, G. Breiner, G. Wang, D. A. Dickie, A. Molino, J. L. Dutton, D. J. D. Wilson, R. J. Gilliard, *Inorg. Chem.* **2019**, *58*, 11118–11126.
[46] L. A. Freeman, J. E. Walley, D. A. Dickie, R. J. Gilliard, *Dalton Trans.* **2019**, *48*, 17174–17178.
[47] M. Wiesinger, B. Maitland, H. Elsen, J. Pahl, S. Harder, *Eur. J. Inorg. Chem.* **2019**, 4433–4439.
[48] M. Arrowsmith, M. S. Hill, D. J. MacDougall, M. F. Mahon, *Angew. Chem. Int. Ed.* **2009**, *48*, 4013–4016; *Angew. Chem.* **2009**, *121*, 4073–4076.
[49] K. J. Sabourin, A. C. Malcolm, R. McDonald, M. J. Ferguson, E. Rivard, *Dalton Trans.* **2013**, *42*, 4625–4632.
[50] N. L. Oldroyd, S. S. Chitnis, V. T. Annibale, M. I. Arz, H. A. Sparkes, I. Manners, *Nat. Commun.* **2019**, *10*, 1370.
[51] N. E. Stubbs, T. Jurca, E. M. Leitao, C. H. Woodall, I. Manners, *Chem. Commun.* **2013**, *49*, 9098–9100.
[52] A. C. Malcolm, K. J. Sabourin, R. McDonald, M. J. Ferguson, E. Rivard, *Inorg. Chem.* **2012**, *51*, 12905–12916.
[53] A. J. Boutland, A. Carroll, C. Alvarez Lamsfus, A. Stasch, L. Maron, C. Jones, *J. Am. Chem. Soc.* **2017**, *139*, 18190–18193.
[54] A. D. Obi, L. A. Freeman, D. A. Dickie, R. J. Gilliard, *Organometallics* **2020**, *39*, 4575–4583.
[55] J. E. Walley, Y.-O. Wong, L. A. Freeman, D. A. Dickie, R. J. Gilliard, *Catalysts* **2019**, *9*, 934–945.
[56] J.-C. Bruyere, C. Gourlaouen, L. Karmazin, C. Bailly, C. Boudon, L. Ruhlmann, P. de Frémont, S. Dagorne, *Organometallics* **2019**, *38*, 2748–2757.
[57] A. R. Kennedy, R. E. Mulvey, S. D. Robertson, *Dalton Trans.* **2010**, *39*, 9091–9099.
[58] N. Kuhn, T. Kratz, *Synthesis* **1993**, *1993*, 561–562.
[59] Deposition Numbers 2171705, 2171706, 2171707, 2171708, 2171709, 2171710, 2171711, 2171712, 2171713, 2193394, 2193395, and 2193396 contain the supplementary crystallographic data for this paper. These data are provided free of charge by the joint Cambridge Crystallographic Data Centre and Fachinformationszentrum Karlsruhe Access Structures service.
[60] ^{iPr}NHC–BN was independently prepared from the reaction of $[Me_2NBH_2]_2$ and ^{iPr}NHC (80 °C, 2 h, and fully characterized by heteronuclear NMR and X-ray crystallography. See Supporting Information for details.
[61] A. Jana, C. Schulzke, H. W. Roesky, *J. Am. Chem. Soc.* **2009**, *131*, 4600–4601.
[62] W. A. Herrmann, O. Runte, G. Artus, *J. Organomet. Chem.* **1995**, *501*, C1–C4.
[63] K. Yuvaraj, I. Douair, A. Paparo, L. Maron, C. Jones, *J. Am. Chem. Soc.* **2019**, *141*, 8764–8768.
[64] H. C. Johnson, A. P. M. Robertson, A. B. Chaplin, L. J. Sewell, A. L. Thompson, M. F. Haddow, I. Manners, A. S. Weller, *J. Am. Chem. Soc.* **2011**, *133*, 11076–11079.
[65] J.-D. Chai, M. Head-Gordon, *Phys. Chem. Chem. Phys.* **2008**, *10*, 6615–6620.
[66] T. H. Dunning Jr., *J. Chem. Phys.* **1989**, *90*, 1007–1023.
[67] R. A. Kendall, T. H. D. Jr, R. J. Harrison, *J. Chem. Phys.* **1992**, *96*, 6796–6806.
[68] K. A. Peterson, *J. Chem. Phys.* **2003**, *119*, 11099–11112.
[69] K. A. Peterson, D. Figgen, E. Goll, H. Stoll, M. Dolg, *J. Chem. Phys.* **2003**, *119*, 11113–11123.
[70] K. A. Peterson, B. C. Shepler, D. Figgen, H. Stoll, *J. Phys. Chem. A* **2006**, *110*, 13877–13883.
[71] V. Butera, N. Russo, E. Sicilia, *Chem. Eur. J.* **2014**, *20*, 5967–5976.

Manuscript received: August 4, 2022
Accepted manuscript online: August 24, 2022
Version of record online: September 12, 2022

© 2022 Wiley-VCH GmbH

15213773, 2022, 43, Downloaded from https://onlinelibrary.wiley.com/doi/10.1002/anie.202211496 by Mississippi State University, Wiley Online Library on [26/06/2023]. See the Terms and Conditions (https://onlinelibrary.wiley.com/terms-and-conditions) on Wiley Online Library for rules of use; OA articles are governed by the applicable Creative Commons License